LA-UR- 92-3057

Title: THE LOCAL STRUCTURE OF HIGH-TEMPERATURE SUPERCONDUCTORS

LA-UR--92-3057

DE93 000653

Author(s): Jose Mustre-de Leon
Steven D. Conradson
Alan R. Bishop
Ian D. Raistrick

Submitted to: 7th International Conference on X-Ray Absorption Fine Structure

MASTER

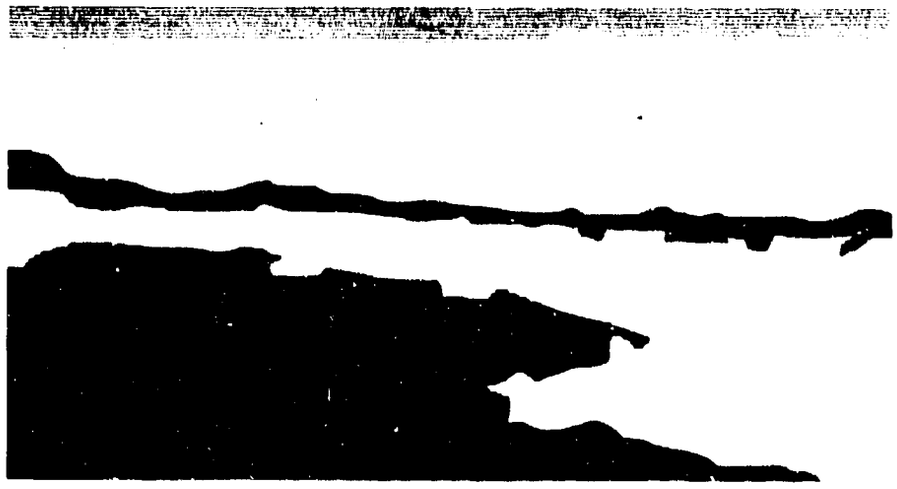

Los Alamos
NATIONAL LABORATORY

Form No. 836 R5
ST 2629 10/91

The Local Structure of High-Temperature Superconductors

José MUSTRE DE LEON, Steven D. CONRADSON, Alan R. BISHOP, and Ian D. RAISTRICK
Los Alamos National Laboratory, Los Alamos, New Mexico 87545, USA

We show how XAFS has been successfully used in the determination of the local crystal structure of high-temperature superconductors, with advantages over traditional diffraction techniques. We review the experimental results that yielded the first evidence for an axial-oxygen-centered lattice instability connected with the superconductivity transition. The interpretation of this instability in terms of a dynamical tunneling model suggests the presence of polarons in these materials. XAFS on $Tl_2Ba_2CuO_6$ and other Tl-based superconductors indicate the presence of local instabilities in the CuO_2 planes of these materials, in addition to axial-oxygen instabilities.

1. Introduction

Six years after the discovery of high-temperature superconductivity the microscopic origin of the pairing mechanism is still not clear. However, several experiments have shown evidence for strong coupling between the lattice and the electrons that take part in the superconductivity, suggesting the importance of the electron-phonon interaction in addition to the electron-electron interaction in understanding the origin of high-temperature superconductivity. This strong interaction does not produce noticeable changes in the average crystalline structure (probed by diffraction). However, it gives rise to changes in the local crystalline structure in the vicinity of the superconducting transition. Such changes have been studied, indirectly, by optical spectroscopy, through the temperature dependence of the relevant local vibrational modes.[1] The local structure has also been probed *directly* using local techniques such as: ion-channeling,[2] pair distribution function analysis of neutron scattering,[3] Mössbauer spectroscopy[4] and XAFS.[5]

Among these local probes, XAFS provides a direct measurement of pair radial distribution functions, it being able to resolve details on a scale given by $\Delta R \approx 1/k_{max}$, where k_{max} is the maximum value of the photoelectron momentum probed in the experiment. We note that the equivalent variable to the photoelectron momentum in pair-distribution function (PDF) analysis of neutron scattering is the momentum transfer $q=2k$. Consequently, to achieve the same resolution in real space in a neutron scattering experiment as that achieved in XAFS it is necessary to use a value of q twice that of k_{max}. In addition, conventional Rietveld refinements of diffraction data, used to determine crystalline structure, assume a particular symmetry group. While the average structure is consistent with the assumed symmetry group, *locally* such symmetry might be broken. In contrast, in XAFS the determination of the pair distribution function does not assume a particular symmetry.[6] This limitation made it impossible to observe the double-well axial-oxygen lattice instability determined by XAFS[5] using conventional neutron and x-ray diffraction.

In section 2 we review the XAFS formulation expressed in terms of pair radial distribution functions (RDFs), determined from model pair potentials. We also discuss the advantage of XAFS over PDF analysis of neutron scattering data in discerning details of the RDF. In section 3 we summarize the main results regarding the RDF for the Cu-axial oxygen pairs in $YBa_2Cu_3O_{7-\delta}$ and $TlBa_2Ca_3Cu_4O_{11}$. In section 4 we present the results of a Peierls-Hubbard model, which shows an underlying polaronic origin for the double-peaked Cu-axial oxygen RDF. In section 5 we show results supporting the existence of a multisite RDF for the Cu-O bonds in the CuO_2 planes of $Tl_2Ba_2CuO_6$. We present the conclusions of this paper in section 6.

2. Pair radial distribution functions and XAFS

We have presented a general discussion of the relation between XAFS and the RDF elsewhere,[7] here we give a summary of the method.

For a many body system we compute the XAFS at finite temperature by forming the statistical average:

$$\langle \chi \rangle = \mathrm{Tr}[\rho\chi]. \tag{1}$$

Here, ρ denotes the density matrix associated with the many body Hamiltonian, $H(\{q_i\},\{p_i\})$, which involves the coordinates, $\{q_i\}$, and momenta, $\{p_i\}$, of all the ions in the system. For simplicity, we assume that χ is given by the K-edge single scattering XAFS formula for unpolarized x-rays incident on a polycrystalline sample:

$$\chi(k,r) = -\mathrm{Im}\left[B(k,r)\frac{\exp(2ikr + i\phi(k,r)}{kr^2} \right], \tag{2}$$

where, r is the bond vector between the absorbing and scattering atoms. The photoelectron wavenumber, k, is referenced to an arbitrary energy reference, E_0. $B(k,r)$ is the (complex) scattering factor associated with both the backscattering process and the presence of the absorbing atom potential.[8]

In the single particle approximation this average can be expressed in terms of a RDF, $g(r)$,

$$\langle \chi \rangle = \int dr g(r)\chi(k,r(r)). \tag{3}$$

The RDF represents the probability distribution of finding a given atomic pair separated by a distance r. If one assumes that the physical origin of this distribution is solely due to

the thermal motion of the atoms, then $g(z)$ is given in terms of the single-particle wave functions, $\{\Psi_i(z)\}$, where z denotes the relative displacement along the bond direction;

$$g(z) = \frac{\sum_i |\Psi_i(z)|^2 e^{-\beta\varepsilon_i}}{\sum_i e^{-\beta\varepsilon_i}} . \qquad (4)$$

Here, ε_i denotes the i^{th} eigenvalue of the single particle Hamiltonian, and the temperature of the system enters through $\beta = 1/k_B T$. We determine the wave functions by solving the Schrödinger equation using the reduced mass, m, for the atomic pair of interest, and a model potential $V(z)$, characterized by parameters determined by fitting to experimental data. Since the variation of the XAFS phase and amplitude functions is small in the region of interest of the ionic motion, one can use XAFS amplitudes and phases derived from reference systems.[8]

Eqs. 3 and 4 represent the average of χ for the general case of a quantum mechanical system at finite temperature. Given this average, we perform a nonlinear least-squares fit between $<\chi>$ and experimental data in the k region of interest, using, as parameters to be determined, the average bond length, R, and the parameters entering in the definition of $V(z)$. The number of atoms, N, is held fixed at the value determined by crystallography.

We note that the parameterization of $g(z)$ provides a natural way to study non-gaussian static disorder. In this case, one can still use Eq. 3, with $g(z)$ characterized in terms of parameters determined by fitting Eq. 3 to experimental data.

As shown by Eq. 3 XAFS provides a direct measurement of the RDF for a given pair of atoms. More precisely, the integral in Eq. 3 shows that $<\chi>$ is a convolution of the RDF and the scattering factors entering in Eq. 2. Consequently, any errors in the estimation of these factors will result will result in corresponding errors and ambiguities in the determination of $g(z)$.

Pair distribution function (PDF) analysis of neutron (or x-ray) diffraction data also probes the RDF of a given pair of atoms. However, this technique is commonly used in *unoriented* powder samples, leading to a PDF which consists of an average of the RDF's for all different pairs and over all angles, convoluted with the neutron scattering factor for each different atom. In this sense XAFS on *oriented* samples provides a more direct probe of the RDF for a given pair, as long as multiple scattering is not significant. Consequently, for determination of local structure over the scale $R < 4$ Å, XAFS is a more sensitive technique than PDF, while for determination of local structure over the range $4 < R < 40$ Å PDF analysis is more sensitive than XAFS.[3,9]

3. The Cu-axial oxygen radial distribution function

Polarized XAFS measurements separate the Cu axial oxygen (O(4)) contributions from those arising from Cu-equatorial oxygen bonds. This is particularly important in $YBa_2Cu_3O_7$, where the Cu(1)-O(4) bond length is similar to the Cu-equatorial oxygen distances. Because of these overlaps, the analysis of unpolarized data can yield to ambiguities in quantitative analysis of the Cu(1)-O(4) RDF.[10]

We analyzed the Cu-O(4) contributions to the polarized ($\vec{E} \parallel c$) Cu K edge XAFS for temperatures 10 K < T < 105 K. Qualitatively, the change of the local structure can be observed in the Fourier transform of the data, where the Cu-O(4) contributions show a single peaked structure for 83 and 86 K and a double peaked structure for other temperatures.[7] The difference in the spectra at different temperatures is more explicit in the isolated Cu-O(4) contribution (obtained by back transforming over the region $1.1 < R < 2.0$ Å), where the presence of a beat around $k = 12$ Å^{-1} signals two Cu(1)-O(4) distances. This beat disappears for temperatures near the superconducting transition temperature T_c. The contribution from the softer Cu(2)-O(4) bond is negligible in the beat region.[7]

Quantitative information about the Cu-O(4) RDF was extracted by nonlinear least-squares fitting over the range $3 < k < 14$ Å^{-1}, on Fourier-filtered data measured at $T = 10$, 83, 86, 88, 95, and 105 K. We included both Cu(1)-O(4) and Cu(2)-O(4) contributions and assumed a double-well parabolic potential of the form;

$$V(z) = \begin{cases} (a/2)(z - z_1)^2 , & z \le z_0 \\ (b/2)(z - z_2)^2 , & z \ge z_0 \end{cases} , \qquad (5)$$

where a, b, z_1, z_2 are determined by the fit. The RDF resulting from the fits is shown in Fig. 1.

We found that $g(z)$ exhibits two peaks separated by 0.13 Å for temperatures $T = 10$ K, and $T > 86$ K, with a decrease in the separation of ~ 0.2 Å inside a fluctuation region around T_c. We note that the actual temperatures of the sample are 5-10 K higher than those quoted here. This change in $g(z)$ is the result of a change in the potential $V(z)$ as shown in Fig. 1. The motion of the O(4) atom in the deep-double-well potential, $V(z)$, can be described by a two-level system, with a symmetric ground state and an antisymmetric first excited state, separated by an energy $\hbar\omega_T = \varepsilon_1 - \varepsilon_2$, where ω_T is the tunneling frequency between the two well minima. The change in $g(z)$ can be conveniently characterized by the change in ω_T as shown in Fig. 2. We have explained this behavior by assuming a coupling between the proposed two-level system and the superconducting order parameter (including fluctuations).[6]

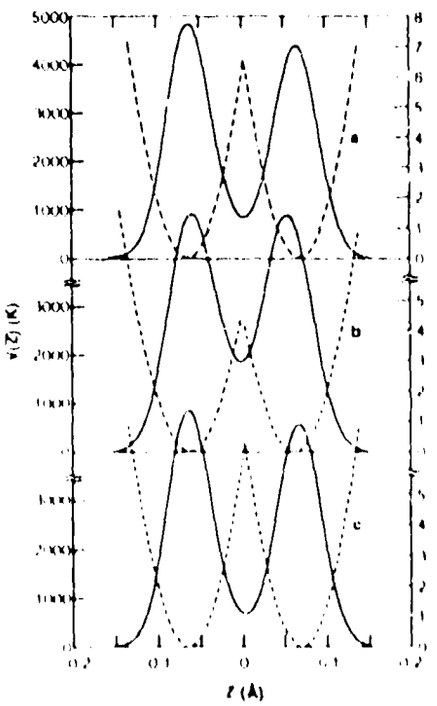

Fig. 1. Radial distribution function $g(z)$ (solid line) and potential $V(z)$ (in units of 10^3 K) for (a) $T = 10$ K, (b) $T = 86$ K, and (c) $T = 105$ K.

We also studied the Cu-O(4) contributions to the polarized ($\varepsilon \parallel c$) Cu K-edge XAFS in $YBa_2Cu_3O_{6.5}$, $YBa_2Cu_{2.8}Co_{0.2}O_7$, at 10 K, using a nonlinear least-squares fit as described above. In this case we found a systematic decrease of the tunneling frequency ω_T as a function of T_c.[11] We interpreted this trend as an indication that the motion of the O(4) atom becomes more *harmonic* with decreasing T_c. Besides the YBCO system, we have studied Tl-based materials. We analyzed *unpolarized* Cu-K edge XAFS data from $TlBa_2Ca_3Cu_4O_{11}$. In this material the absence of a short Cu-axial oxygen bond allowed us to separate the Cu-axial oxygen contributions from the Cu-equatorial oxygen contributions, making it possible to use XAFS data from unoriented powders to study the Cu-axial oxygen RDF. In this case it was not possible to use the formalism based on a potential as described above (due to the inapplicability of the Einstein formalism for the long Cu-O bond). Nonlinear least-square fits using gaussian peaks show two Cu-axial oxygen positions separated by 0.17 Å, with the separation decreasing to less than 0.10 Å within a fluctuation region around T_c.[12] This finding is consistent with the observation of a split axial oxygen position in $Tl_2Ba_2CaCu_2O_8$ by PDF analysis of neutron *inelastic* scattering, supporting the *dynamical* interpretation of the XAFS results in terms of a pair-potential. The finding of a split axial-oxygen position in Tl-based materials suggests that this might be a general characteristic of high-temperature superconductors. Recently, Bianconi *et al.* have found evidence for a split axial oxygen position in Bi-based materials,[13] which they have connected with the motion of holes in this atom.

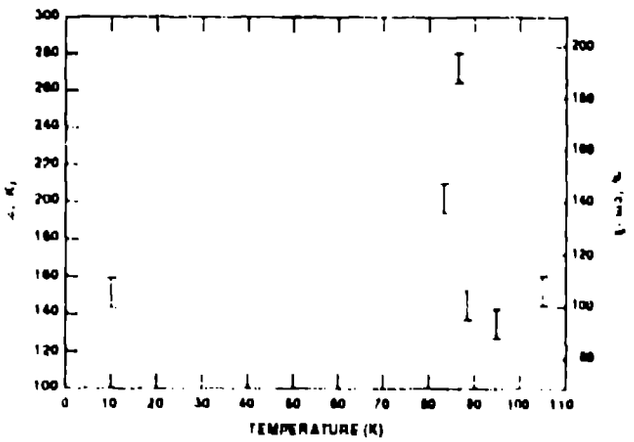

Fig. 2 Tunneling frequency, ω_T between the two O(4) sites, as a function of temperature in $YBa_2Cu_3O_7$

4. Polaronic origin of the Cu-axial oxygen RDF

The analysis of the Cu O(4) XAFS in terms of a *static* potential describes adequately the structure and dynamical origin of the RDF. However, these XAFS experiments are not designed to probe the excited vibrational states. Consequently, the potential $V(r)$ is not expected to describe in adequate manner these excited vibrational levels. Specifically, anomalies similar to those observed in the tunneling frequency, ω_T should be present in the Raman and infrared active modes associated with the Cu O(4) vibrations. However, the direct use of the potential, $V(r)$, to calculate the expected results for these spectroscopies is not adequate.[6] In fact, the 505 cm^{-1} A_1 Raman active mode in $YBa_2Cu_3O_7$ shows a hardening near T_c, while the associated 585 cm^{-1} infrared active mode softens over the same temperature region. Both of these "anomalies" are only ~ 2-3% in contrast to the 80% anomaly in the tunneling frequency derived from XAFS.

We considered a Peierls-Hubbard model, representing c-axis charge transfer, including both infrared active and Raman vibrations in the isolated O(4)-Cu(1)-O(4) cluster. This model allowed us to: i) understand the origin of the differing behavior of the infrared and Raman modes, ii) understand the *quantitative* difference between the anomaly in the tunneling frequency derived from XAFS, and the anomalies in the frequencies of the Raman and infrared active modes, and iii) show an underlying polaronic origin for the two-site Cu(1)-O(4) RDF.

The Hamiltonian is given by:

$$H = H_{el} + H_{ph} + H_{el-ph} \quad (6)$$

$$H_{el} = \sum_{\sigma,i=1}^{3} \varepsilon_i n_{i,\sigma} + \sum_{i=1}^{3} U n_{i\uparrow} n_{i\downarrow} + t' \sum_{\sigma} c^{\dagger}_{1,\sigma} c_{2,\sigma} + c^{\dagger}_{2,\sigma} c_{1,\sigma} + \text{h.c.} \quad (6a)$$

$$H_{ph} = \hbar\omega^0_R b^{\dagger}_R b_R + \hbar\omega^0_{IR} b^{\dagger}_{IR} b_{IR} \quad (6b)$$

$$H_{el-ph} = \lambda_R u_R \sum_{\sigma} (n_{1\sigma} - 2n_{2\sigma} + n_{3\sigma}) + \lambda_{IR} u_{IR} \sum_{\sigma} (n_{3\sigma} - n_{1\sigma}) \quad (6c)$$

Here, $n_{i\sigma} = c^{\dagger}_{i\sigma} c_{i\sigma}$ denotes the number operator for holes of spin σ at site i; i=1,3 indicating the lower (upper) O(4) site, and i=2 the Cu(1) site, with site energies ε_i, hopping amplitude t, and on-site repulsion U. The phonon part of the Hamiltonian (6b) consists of harmonic Raman and infrared oscillators with creation operators $b_R^{\dagger}$ and $b_{IR}^{\dagger}$ and bare frequencies ω_R^0, ω_{IR}^0, respectively. The interaction term (6c) reflects the fact that for added holes at the Cu(1) site the Cu(1)-O(4) attraction is strengthened, while for holes added at the O(4) sites the attraction is weakened, favoring a longer Cu(1)-O(4) bond length. We note that in this model anharmonicity is *not* present in the phonon Hamiltonian, but is generated by sufficiently strong *linear* electron phonon coupling. We assumed two holes of different spin, leading to the cluster states: a) $O(4)^2\ Cu(1)^{2+}\ O(4)^2$, b) $O(4)^1\ Cu(1)^{3+}\ O(4)^2$, consistent with XANES results. The state $O(4)^1\ Cu(1)^{3+}\ O(4)^1$ is found to be important as an intermediate state for tunneling between states a) and b).

We carried out an exact diagonalization of this model, finding that the coupling between c-axis phonons and charge transfer between Cu(1) and O(4) ions generates a double well for the 585 cm^{-1} infrared active mode, while it leads to a shifted single well for the associated Raman mode, for strong enough electron phonon coupling (Fig. 3). This result is consistent with the nearly symmetric Cu(1)-O(4) RDF obtained from the XAFS analysis, indicating that the double peaked RDF reflects the degenerate ground state for the infrared mode.[6] This picture reconciles the apparent discrepancy between optical and structural (XAFS) observations. The model predicts multiphonon and nonadiabatic effects, not contained in lattice dynamics calculations that use *static* anharmonic potentials. This calculation also [illegible]

double-peaked Cu(1)-O(4) RDF has a polaronic origin - the hole location follows the lattice distortion in the O(4)-Cu(1)-O(4) cluster.[9]

5. In-plane Cu-O anomalies in Tl-based superconductors

YBCO is an ideal system to study details of the Cu-O(4) RDF using XAFS, due to the short Cu(1)-O(4) bond length. However the presence of the Cu(1)-O(1) chains, makes it difficult to separate the XAFS contributions from these chains and the Cu-O bonds in the CuO_2 planes. Consequently, we have used Tl-based compounds with well-characterized average crystalline structure,[15] to study the local structure of the CuO_2 planes.

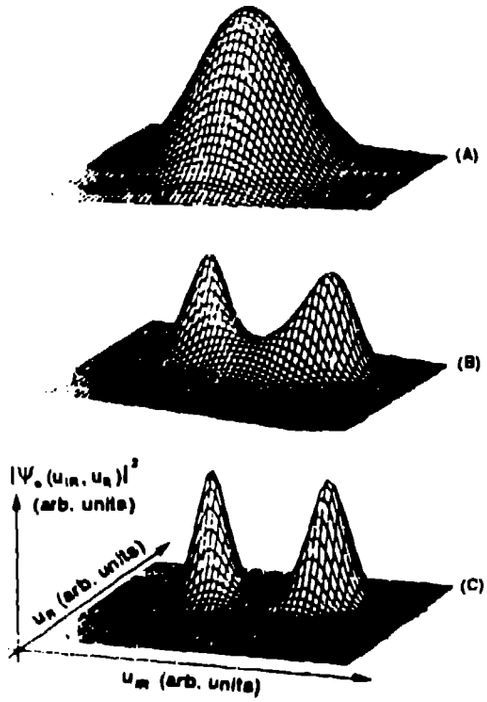

Fig. 3. Squared many body ground state wavefunction of the O(4) Cu(1) O(4) cluster as a function of the Raman (u_R) and infrared (u_{IR}) coordinates for λ_{IR} = a) 0.10, b) 0.12, c) 0.15 (in all cases λ_R 0.10)

We have found evidence for: i) changes in the Cu-equatorial oxygen bonds across T_c, ii) a multisite RDF for the Cu-equatorial oxygen bonds, and iii) the existence of a double-peaked RDF for the Cu-axial oxygen bond, in agreement with our results in other materials.

We analyzed the Cu K edge XAFS on *unoriented* powders of $Tl_2Ba_2CuO_6$ (T_c = 89 K) and $Tl_2Ba_2CaCu_2O_8$ (T_c = 105 K), collected at several temperatures across their respective T_c. Details of the analysis will be published elsewhere.[16] Here, we summarize some of the major results as indicated above.

Qualitatively, the change in the local structure of the CuO_2 planes is reflected in the Fourier transform of the spectra. While, the Cu-Ba and Cu-Cu peaks exhibit the expected decrease and broadening with increasing temperature, the peak associated with the Cu-equatorial oxygen bonds shows a higher and narrower profile for temperatures in the vicinity of T_c, compared with the profile at low temperatures (T = 10 K) or temperatures above T_c. Curve fits of the isolated Cu-equatorial oxygen contribution in k-space over a narrow range ($3 < k < 10$ Å^{-1}) using a *single-gaussian* RDF indicate a *decrease* in the Debye-Waller factor for temperatures near T_c. This finding proves the existence of a strong coupling between the phonons associated with the CuO_2 planes and the superconducting electrons.

Fits to the isolated Cu-equatorial oxygen contribution in k-space over a longer range ($3 < k < 13$ Å^{-1}) show the inadequacy of a single-site RDF to fit these data. A double-peaked RDF leads to better agreement with experiment, indicating a distribution of distances in the range $1.87 < R < 1.98$ Å. The presence of a *short* Cu-equatorial oxygen distance, R = 1.87 Å, indicates that the equatorial oxygen must be displaced off-center along the Cu-Cu bond, leading to a short and a long Cu-O distance. A distortion of the Cu-O bond in the c-directions is also possible (such a distortion has been proposed by Bianconi *et al.* in Bi based compounds[13]).

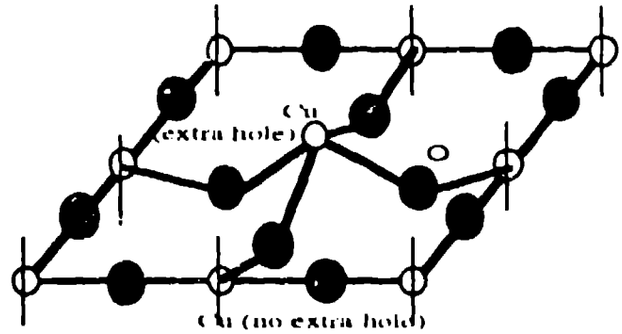

Fig. 4. Proposed local structure of the CuO_2 planes in high temperature superconductors

We propose that this distortion is correlated with the *two* positions found for the axial oxygen, and reflects the presence of extra holes at selected Cu sites leading to the structure shown in Fig. 4. We are currently studying XAFS on oriented $Tl_2Ba_2CuO_6$ powders to characterize quantitatively this distortion and its correlation with axial oxygen distortion.

6. Conclusions

We have presented several XAFS results that show a coupling between the lattice and the superconducting electrons in high-temperature superconductors. This coupling manifests itself as a change in the local structure of these materials in the vicinity of T_c. The existence of multisite RDF's suggests the presence of polarons in these materials.

Acknowledgments

P. G. Allen, J. Batistic, F. H. Garzon, G. G. Li, M. A. Subramanian, and S. A. Trugman have also been involved at different stages of this work. We are grateful to S. Sampson for a critical review of this manuscript. Experiments were carried out at SSRL. We would like to thank the Advanced Computing Laboratory at Los Alamos for the use of a CONVEX C-220 computer in the theoretical calculations. This work was funded by the Basic Energy Science office of the Department of Energy.

References

1) B. Friedl, C. Thomsen, and M. Cardona. Phys. Rev. Lett. 65, (1990) 915 ; H.S. Obhi and E.K. Salje: Physica C 171 (1990) 547.

2) R.P. Sharma, L.E. Rehn, P. M. Baldo, and J. Z.Liu: Phys. Rev. Lett. 62 (1989) 2869.

3) B. H. Toby , T. E. Egami, J. D Jorgen :en, and M. A. Subramanian: Phys. Rev. Lett. 64 (1990), 2414

4) Y. Wu, S. Pradhan, and P. Boolchand: Phys. Rev Lett. 67 (1991) 4184.

5) S. D. Conradson, I. D. Raistrick, and A. R. Bishop: Science 248 (1990) 1394; J. Mustre de Leon, S. D. Conradson, I. Batistic, and A. R Bishop: Phys. Rev. Lett. 65 (1990) 1675.

6) J. Mustre de Leon, I. Batistic, A. R. Bishop, S. D. Conradson, and S. A. Trugman: Phys. Rev. Lett. 68 (1992) 3236.

7) J. Mustre de Leon, S. D Conradson, I. Batistic, A. R Bishop, I. D. Raistrick, M. C. Aronson, and F. H. Garzon: Phys. Rev B 45 (1992) 2447.

8) J. J. Rehr, J Mustre de Leon, R C. Albers, and S. I. Zabinsky: J Am. Chem. Soc. 113 (1991) 5135; J. Mustre de Leon, J. J. Rehr, R. C Albers, and S. I. Zabinky: Phys. Rev. B 44 (1991) 4146.

9) S. J. L. Billinge, P. K. Davies, T. Egami, and C. R. A. Catlow: Phys. Rev. B 43 (1991) 10340.

10) J. Röhler: Lattice effects in High temperature Superconductors, eds. Y. Bar-Yam, T. Egami, J. Mustre de Leon, and A.R. Bishop (World Scientific, Singapore, 1992), in press.

11) J. Mustre de Leon , S D. Conradson, I. Batistic, and A. R. Bishop: Phys Rev. B 44 (1991) 2422

12) P. G Allen, J. Mustre de Leon, S. D. Conradson, and A. R. Bishop: Phys. Rev. B 44 (1991) 9480.

13) A. Bianconi , S Della Longa, M. Missori, I. Pettiti, and M. Pompa. Lattice effects in High temperature Superconductors, eds. Y Bar-Yam, T. Egami, J. Mustre de Leon, and A R. Bishop (World Scientific, Singapore, 1992), in press.

14) J. Mustre de Leon, S D Conradson, P. G. Allen, I Batistic, and A. R Bishop High Temperature Superconductivity, eds J. Ashkenazi *et al.* (Plenum Press, New York 1991), pg. 425

15) C C Torardi, M A Subramanian, J. C. Calabrese, J. Gopalakrishnan, E M McCarron, K. J Morrissey, T R Askew, R B Flippen, U Chowdhry, and A W Sleight Phys Rev B 38 (1988) 225.

16) G G Li, J Mustre de Leon, S D Conradson, A R Bishop, M A Subramanian, and I D Raistrick in preparation